

# **SYNTHESIS AND CHARACTERIZATION OF POLYANILINE, GRAPHENE AND GRAPHENE/POLYANILINE NANOCOMPOSITES**

**CHIN SEIK YEE**

**UNIVERSITI SAINS MALAYSIA**

**2018**

**SYNTHESIS AND CHARACTERIZATION OF POLYANILINE, GRAPHENE  
AND GRAPHENE/POLYANILINE NANOCOMPOSITES**

**by**

**CHIN SEIK YEE**

**Thesis submitted in fulfilment of the  
requirements for the degree of  
Master of Science**

**August 2018**

## **ACKNOWLEDGEMENT**

First of all, I would like to take this opportunity to thank School of Materials and Mineral Resources Engineering, Universiti Sains Malaysia for offering me the Master program. I would like to express my deepest appreciation to my supervisor, Prof. Ir. Dr. Mariatti Jaafar, who led me into the interesting research topic of graphene. Without her great mentorship, invaluable guidance, and helpful advice, this thesis could not have been completed. I have learnt a lot of new knowledge during completion of this Master project. I would also like to thank my co-supervisor, Dr. Tuti Katrina for her help to complete my project.

Secondly, I would like to express my profound gratitude to the Dean, Prof. Dr. Zuhailawati Hussain, for providing me all necessary facilities during my research work. I would like to acknowledge the technical support to all the laboratory technicians for their valuable help.

Besides, I would like to extend my thanks to Ministry of Education (MOE) for awarding Fundamental Research Grant (Grant, no. 6071284) that made this research possible. Also, special thanks to Ministry of Higher Education (MOHE) for awarding My Brain 15 (under My Master scheme) sponsorship throughout the Master study.

Lastly, I would like to give my heartfelt thanks to my friends for helping me the relevant and useful information in the process of completing this project. I am heartily thankful to my beloved parents and family members for their unconditional love and financial support.

## TABLE OF CONTENTS

|                       | Page |
|-----------------------|------|
| ACKNOWLEDGEMENT       | ii   |
| TABLE OF CONTENTS     | iii  |
| LIST OF TABLES        | viii |
| LIST OF FIGURES       | x    |
| LIST OF SYMBOLS       | xvi  |
| LIST OF ABBREVIATIONS | xvii |
| ABSTRAK               | xix  |
| ABSTRACT              | xx   |

## CHAPTER ONE: INTRODUCTION

|     |                        |   |
|-----|------------------------|---|
| 1.1 | Background of Research | 1 |
| 1.2 | Problem Statement      | 5 |
| 1.3 | Research Objectives    | 7 |
| 1.4 | Thesis Outline         | 8 |

## CHAPTER TWO: LITERATURE REVIEW

|       |  |    |
|-------|--|----|
| 2.1   | Introduction   | 9  |
| 2.1.1 | Introduction to Graphene                                     | 9  |
| 2.2   | Synthesis methods for graphene production                    | 12 |
| 2.2.1 | Micromechanical Cleavage of Graphite (Scotch Tape Technique) | 15 |

|       |   |    |
|-------|---|----|
| 2.2.2 | Chemically derived graphene from graphene oxide                 | 16 |
| 2.2.3 | Chemical Vapour Deposition                                      | 18 |
| 2.2.4 | Electrochemical exfoliation                                     | 20 |
| 2.3   | Characterization method for graphene                            | 23 |
| 2.3.1 | Electron microscopy   | 23 |
| 2.3.2 | X-ray diffraction analysis                                      | 26 |
| 2.3.3 | Fourier transform infrared spectroscopy analysis                | 28 |
| 2.3.4 | X-ray photoelectron spectroscopy analysis                       | 29 |
| 2.3.5 | Raman spectroscopy analysis                                     | 31 |
| 2.4   | Applications  | 33 |
| 2.5   | Conducting polymers   | 34 |
| 2.6   | Polyaniline (PANI)  | 36 |
| 2.7   | Nanostructured polyaniline                                      | 38 |
| 2.8   | Solubility of PANI  | 41 |
| 2.9   | Graphene/Polymer Nanocomposites                                 | 43 |
| 2.9.1 | Conductive filler filled insulating polymer composites          | 44 |
| 2.9.1 | Conductive filler filled insulating polymer composites          | 45 |
| 2.10  | The challenge of graphene application in polymer nanocomposites | 46 |

## **CHAPTER THREE: MATERIALS AND METHOD**

|     |             |    |
|-----|-------------|----|
| 3.1 | An Overview | 52 |
|-----|-------------|----|

|       |  |    |
|-------|--|----|
| 3.2   | Materials and chemicals                                  | 52 |
| 3.2.1 | Working electrode  | 52 |
| 3.2.2 | Electrolyte  | 53 |
| 3.2.3 | Monomer  | 54 |
| 3.2.4 | Oxidant  | 55 |
| 3.2.5 | Surfactant   | 55 |
| 3.2.6 | Other chemicals  | 56 |
| 3.3   | Sample preparation                                       | 56 |
| 3.3.1 | Synthesis of PANI using conventional polymerization      | 57 |
| 3.3.2 | Synthesis of PANI using interfacial polymerization       | 58 |
| 3.3.3 | Synthesis of graphene though electrochemical exfoliation | 59 |
| 3.3.4 | One-step synthesis of graphene/PANI-SDBS nanocomposites  | 60 |
| 3.4   | Characterizations  | 62 |
| 3.4.1 | Scanning electron microscopy                             | 62 |
| 3.4.2 | Transmission electron microscopy analysis                | 62 |
| 3.4.3 | X-ray Diffraction  | 63 |
| 3.4.4 | X-Ray Photoelectron Spectroscopy                         | 63 |
| 3.4.5 | Fourier transform infrared spectroscopy                  | 64 |
| 3.4.6 | Raman spectroscopy                                       | 64 |
| 3.4.7 | Ultraviolet-visible spectroscopy analysis                | 64 |
| 3.4.8 | Thermogravimetric analysis                               | 65 |
| 3.4.9 | Electrical conductivity                                  | 65 |

## **CHAPTER FOUR: RESULTS AND DISCUSSION**

|       |  |     |
|-------|--|-----|
| 4.1   | Synthesis of PANI and PANI-SDBS                      | 66  |
| 4.1.1 | Morphology   | 66  |
| 4.1.2 | X-ray diffraction analysis                           | 69  |
| 4.1.3 | Fourier transform infrared spectroscopy analysis     | 72  |
| 4.1.4 | Ultraviolet-visible spectroscopy analysis            | 75  |
| 4.1.5 | Thermal properties                                   | 76  |
| 4.1.6 | Electrical conductivity properties                   | 80  |
| 4.2   | Synthesis of graphene by electrochemical exfoliation | 83  |
| 4.2.1 | Dispersion of graphene                               | 83  |
| 4.2.2 | Morphology   | 86  |
| 4.2.3 | X-ray diffraction analysis                           | 91  |
| 4.2.4 | Fourier transform infrared spectroscopy analysis     | 94  |
| 4.2.5 | X-ray photoelectron spectroscopy analysis            | 99  |
| 4.2.6 | Raman spectroscopy analysis                          | 101 |
| 4.2.7 | Ultraviolet-visible spectroscopy analysis            | 103 |
| 4.2.8 | Thermal properties                                   | 104 |
| 4.2.9 | Electrical conductivity properties                   | 106 |
| 4.3   | Synthesis of graphene/PANI-SDBS nanocomposites       | 108 |
| 4.3.1 | Morphology   | 108 |

|       |                                       |     |
|-------|---------------------------------------|-----|
| 4.3.2 | X-ray diffraction analysis            | 111 |
| 4.3.3 | Infrared spectroscopy analysis (FTIR) | 112 |
| 4.3.4 | Ultraviolet-visible analysis          | 114 |
| 4.3.5 | Thermal properties                    | 115 |
| 4.3.6 | Electrical conductivity               | 117 |

## **CHAPTER FIVE: CONCLUSION AND SUGGESTIONS**

|     |                              |     |
|-----|------------------------------|-----|
| 5.1 | Conclusion                   | 120 |
| 5.2 | Suggestions for future works | 122 |

|                   |     |
|-------------------|-----|
| <b>REFERENCES</b> | 123 |
|-------------------|-----|

## **APPENDICES**

Appendix A: Calculation of the crystallize size (L)

Appendix B: Calculation of the number of layers (n)

Appendix C: Calculation of the  $I_D/I_G$  and  $I_{2D}/I_G$  ratio

## **LIST OF PUBLICATIONS**



## LIST OF TABLES

|           |   | <b>Page</b> |
|-----------|---|-------------|
| Table 2.1 | Summary of advantages and disadvantages associated with each graphene production route.                                       | 14          |
| Table 2.2 | The potential applications of conductive materials with regards to the conductivity values.                                   | 49          |
| Table 3.1 | General properties of graphite rod as supplied by manufacturer.   | 53          |
| Table 3.2 | General properties of sulphuric acid as supplied by manufacturer.   | 54          |
| Table 3.3 | General properties of aniline as supplied by manufacturer.  | 54          |
| Table 3.4 | General properties of graphite rod as supplied by manufacturer.   | 55          |
| Table 3.5 | General properties of sodium dodecylbenzenesulfonate as supplied by manufacturer.   | 56          |
| Table 4.1 | Thermal properties of PANI and PANI-SDBS synthesized using different methods.   | 80          |
| Table 4.2 | The crystallite size (L), interlayer spacing (d) and number of layers (n) of the graphene obtained at different applied bias. | 94          |
| Table 4.3 | Thermal properties of graphene obtained at 5V and 10V bias.   | 106         |
| Table 4.4 | Thermal properties of graphene/PANI-SDBS nanocomposites with various amounts of graphene content.                             | 117         |

|           |  |     |
|-----------|--|-----|
| Table 4.5 | Electrical conductivity for PANI, PANI-SDBS and graphene/PANI-SDBS nanocomposites. | 118 |
|-----------|--|-----|

## LIST OF FIGURES

|            |   | <b>Page</b> |
|------------|---|-------------|
| Figure 1.1 | Graphene is a 2D building material for carbon materials of all other dimensionalities (Geim & Novoselov, 2007).   | 2           |
| Figure 2.1 | The illustration of the current preparation methods for graphene (Ambrosi et al., 2014).  | 13          |
| Figure 2.2 | Micromechanical cleavage of graphite. (a) Adhesive tape is pressed against a graphite crystal. (b) The top few layers are attached to the tape. (c) Gently press against a substrate surface of choice. (d) Upon peeling off, the bottom layer is then transferred onto the substrate (Novoselov & Neto, 2012). | 16          |
| Figure 2.3 | Schematic illustration of the graphene oxide by Hummers method (Bai et al., 2011).  | 17          |
| Figure 2.4 | A schematic illustration of the CVD graphene growth on Ni (Al-Shurman & Naseem, 2014).  | 19          |
| Figure 2.5 | SEM and FESEM images of graphene obtained at (a,b) 3V, (c,d) 4.5V and (e,f) 6V (Tiwari et al., 2015).   | 24          |
| Figure 2.6 | (b) SEM image of the exfoliated graphene; (c and d) TEM image and SAED pattern of the exfoliated graphene (Chen & Xue, 2014).   | 25          |
| Figure 2.7 | TEM image (insert: SAED pattern) of FLGNSs obtained at the PA3 and PA4 electrolytic conditions (Sahoo & Mallik, 2015b).   | 26          |
| Figure 2.8 | XRD pattern of graphene using the different oxidising agents (a) nitric acid, (b) sodium nitrate, (c) sulphuric acid and (d) hydrogen peroxide (Hamra et al., 2016).  | 27          |

|             |  |    |
|-------------|--|----|
| Figure 2.9  | FTIR of the pyrolytic graphite sheet (PG), exfoliated few layered graphene at 1.5M (PA3) and 2.0M (PA4) perchloric acid (Sahoo & Mallik, 2015b). | 28 |
| Figure 2.10 | XPS survey scan of the exfoliated graphene at 0.5 M (PA3) and 1.0 M (PA4) perchloric acid (Sahoo & Mallik, 2015b).                               | 30 |
| Figure 2.11 | C 1s spectra of exfoliated graphene prepared with sonication (Liu et al., 2013b).  | 30 |
| Figure 2.12 | Raman spectra of graphene obtained at 3, 4.5 and 6V (Tiwari et al., 2015).   | 32 |
| Figure 2.13 | Applications of graphene-based polymer composites (Das & Prusty, 2013).  | 33 |
| Figure 2.14 | Chemical structure of some CPs (Kaur et al., 2015).  | 35 |
| Figure 2.15 | Different form of PANI structures (Li et al., 2009a)   | 37 |
| Figure 2.16 | Different form of PANI structures (Li et al., 2009a).  | 37 |
| Figure 2.17 | Field Emission Scanning Electron Microscopy (FESEM) image of granular PANI synthesized by conventional method (Abdolahi et al., 2012).           | 39 |
| Figure 3.1  | Chemical structure of sulphuric acid.  | 53 |
| Figure 3.2  | Chemical structure of aniline.   | 54 |
| Figure 3.3  | Chemical structure of ammonium persulfate.   | 55 |
| Figure 3.4  | Chemical structure of sodium dodecylbenzenesulfonate.  | 56 |
| Figure 3.5  | Process flow of the synthesis of PANI using conventional polymerization.   | 57 |

|            |   |    |
|------------|---|----|
| Figure 3.6 | Process flow of the synthesis of PANI using interfacial polymerization.   | 58 |
| Figure 3.7 | A schematic illustration of electrochemical exfoliation of graphite.  | 59 |
| Figure 3.8 | A schematic illustration of one-step interfacial polymerization of graphene/PANI-SDBS nanocomposites.                                     | 60 |
| Figure 3.9 | General flow of the present experimental work.  | 61 |
| Figure 4.1 | FESEM images; (a), (b) PANI and (c), (d) PANI-SDBS at magnifications of (a), (c) 10KX and (b),(d) 30KX using conventional polymerization. | 67 |
| Figure 4.2 | FESEM images; (a), (b) PANI and (c), (d) PANI-SDBS at magnifications of (a), (c) 10KX and (b), (d) 20KX using interfacial polymerization. | 68 |
| Figure 4.3 | XRD patterns of PANI synthesized using (a) conventional and (b) interfacial polymerization.   | 70 |
| Figure 4.4 | XRD patterns of PANI-SDBS synthesized using (a) conventional and (b) interfacial polymerization.  | 71 |
| Figure 4.5 | FTIR spectrum of PANI synthesized using (a) conventional and (b) interfacial polymerization.  | 73 |
| Figure 4.6 | FTIR spectrum of PANI-SDBS synthesized using (a) conventional and (b) interfacial polymerization.   | 74 |
| Figure 4.7 | UV-vis spectra of PANI synthesized using (a) conventional and (b) interfacial polymerization.   | 75 |
| Figure 4.8 | UV-vis spectra of PANI-SDBS synthesized using (a) conventional and (b) interfacial polymerization.  | 76 |

|             |   |    |
|-------------|---|----|
| Figure 4.9  | TGA (i) and DTG (ii) curves of the PANI synthesized using (a) conventional and (b) interfacial polymerization.  | 77 |
| Figure 4.10 | TGA (i) and DTG (ii) curves of the PANI-SDBS synthesized using (a) conventional and (b) interfacial polymerization.   | 79 |
| Figure 4.11 | Electrical conductivity measurements for PANI synthesized using conventional and interfacial polymerization.  | 81 |
| Figure 4.12 | Electrical conductivity measurements for PANI-SDBS synthesized using conventional and interfacial polymerization.   | 82 |
| Figure 4.13 | Photographs of 1mg/mL graphene dispersions in DMF solvent. The photographs were taken at (a) just after sonication, (b) a week after sonication and (c) 3 months later. | 84 |
| Figure 4.14 | Hydrodynamic size distribution of graphene obtained at (a) 5V and (b) 10V bias.   | 85 |
| Figure 4.15 | FESEM images of graphene obtained at (a) 5V and (b) 10V bias at magnifications of 10 KX.  | 87 |
| Figure 4.16 | HRTEM images of graphene obtained at (a) 5V and (b) 10V bias at magnifications of (i) 29KX, (ii) 43KX and (iii) 690 KX.   | 88 |
| Figure 4.17 | SAED pattern of the graphene obtained at (a) 5V and (b) 10V bias.   | 90 |
| Figure 4.18 | XRD patterns of (a) graphite and graphene which obtained at (b) 5V and (c) 10V bias.  | 91 |
| Figure 4.19 | FTIR spectra of graphene obtained at (a) 5V and (b) 10V bias.   | 95 |

|             |  |     |
|-------------|--|-----|
| Figure 4.20 | Schematic illustration of the electrochemical exfoliation of graphite, (a) structure of graphite, (b) oppositely charged ions attack at the edge site and grain boundaries of graphite, (c) the evolution of bubbles, (d) intercalation of negative ions into graphite layer and (e) exfoliation the graphite into graphene. | 98  |
| Figure 4.21 | (a) Wide scan XPS spectra and (b) deconvolution of C1s spectra of graphene obtained at 5V bias.  | 100 |
| Figure 4.22 | Raman spectra of synthesized graphene obtained at (a) 5V and (b) 10V bias.   | 101 |
| Figure 4.23 | UV-vis spectra of graphene obtained at (a) 5V and (b) 10V bias.  | 104 |
| Figure 4.24 | TGA (i) and DTG (ii) curves of graphene obtained at (a) 5V and (b) 10V bias.   | 105 |
| Figure 4.25 | Electrical conductivity of the synthesized graphene obtained at 5V and 10V bias.   | 107 |
| Figure 4.26 | FESEM images; (a) 1 wt% graphene/PANI-SDBS, (b) 3 wt% graphene/PANI-SDBS, (c) 5 wt% graphene/PANI-SDBS nanocomposites and (d) The zoomed-in part of (c) at magnifications of (a), (b), (c) 10KX and (d) 30KX.  | 109 |
| Figure 4.27 | HRTEM images; (a) 1 wt% graphene/PANI-SDBS, (b) 3 wt% graphene/PANI-SDBS, (c) 5 wt% graphene/PANI-SDBS nanocomposites and (d) The zoomed-in part of (d) at magnifications of (a), (b), (c) 43KX and (d) 97KX.  | 110 |
| Figure 4.28 | XRD pattern of (a) 1 wt% graphene/PANI-SDBS, (b) 3 wt% graphene/PANI-SDBS and (d) 5 wt% graphene/PANI-SDBS nanocomposites.   | 111 |
| Figure 4.29 | FTIR spectrum of (a) 1 wt% graphene/PANI-SDBS, (b) 3 wt% graphene/PANI-SDBS and (d) 5 wt% graphene/PANI-SDBS nanocomposites.   | 113 |

|             |   |     |
|-------------|---|-----|
| Figure 4.30 | UV-vis spectra of (a) 1 wt% graphene/PANI-SDBS, (b) 3 wt% graphene/PANI-SDBS and (d) 5 wt% graphene/PANI-SDBS nanocomposites.                                   | 114 |
| Figure 4.31 | TGA (i) and DTG (ii) curves of graphene obtained at (a) 1 wt% graphene/PANI-SDBS, (b) 3 wt% graphene/PANI-SDBS and (c) 5 wt% graphene/PANI-SDBS nanocomposites. | 115 |
| Figure 4.32 | Electrical conductivities as a function of publication year reported of graphene/PANI nanocomposites from the literature.                                       | 119 |



## LIST OF SYMBOLS

|   |                                   |
|---|-----------------------------------|
| 0-D                                     | Zero-dimensional                  |
| 1-D                                     | One-dimensional                   |
| 2-D.                                    | Two-dimensional                   |
| 3-D.                                    | Three-dimensional                 |
| $\text{m}^2\text{g}^{-1}$               | Square meter per gram             |
| $\text{cm}^2\text{V}^{-1}\text{s}^{-1}$ | Square centimeter per volt second |
| TPa                                     | Terapascal                        |
| $\text{Wm}^{-1}\text{K}^{-1}$           | Watts per meter kelvin            |
| $\mu\text{m}^2$                         | Square micron                     |
| $^{\circ}\text{C}$                      | Degree Celsius                    |
| V                                       | Volt                              |
| $2\theta$                               | Two-teta                          |
| $^{\circ}$                              | Degree                            |
| eV                                      | Electronvolt                      |
| S/cm                                    | Siemens per centimetre            |
| $\Sigma$                                | Electrical conductivity           |
| P                                       | Electrical resistivity            |
| %                                       | Percentage                        |
| wt%                                     | Weight percentage                 |
| nm                                      | Nanometers                        |
| $\text{\AA}$                            | Angstrom                          |

## LIST OF ABBREVIATIONS

|                                |  |
|--------------------------------|--|
| APS                            | Ammonium persulfate                              |
| CH <sub>4</sub>                | Methane  |
| CHCl <sub>3</sub>              | Chloroform                                       |
| Cu                             | Copper   |
| CMOS                           | Complementary metal-oxide-semiconductor          |
| CNTs                           | Carbon nanotubes                                 |
| CPs                            | Conducting polymers                              |
| CVD                            | Chemical vapour deposition                       |
| CTAB                           | Cetyltrimethyl ammonium bromide                  |
| ED                             | Electron diffraction                             |
| DBSA                           | Dodecylbenzenesulfonic acid                      |
| DMF                            | Dimethylformamide                                |
| FESEM                          | Field-emission scanning electron microscopy      |
| FTIR                           | Fourier transform infrared spectroscopy          |
| GO                             | Graphene oxide                                   |
| H <sub>2</sub>                 | Hydrogen   |
| HCl                            | Hydrochloric acid                                |
| HNO <sub>3</sub>               | Nitric acid                                      |
| HOPG                           | Highly oriented pyrolytic graphite               |
| HRTEM                          | High-resolution transmission electron microscopy |
| H <sub>2</sub> SO <sub>4</sub> | Sulphuric acid                                   |
| ICPs                           | Intrinsically conducting polymer                 |
| IL                             | Ionic-liquid                                     |
| KClO <sub>3</sub>              | Potassium chlorate                               |
| K <sub>2</sub> SO <sub>4</sub> | Potassium sulfate                                |
| LE                             | Leucoemeraldine                                  |
| NaBH <sub>4</sub>              | Sodium borohydride                               |

|   |                                    |
|---|------------------------------------|
| NaClO <sub>4</sub>                              | Sodium perchlorate                 |
| NaNO <sub>3</sub>                               | Sodium nitrate                     |
| Na <sub>2</sub> SO <sub>4</sub>                 | Sodium sulfate                     |
| N <sub>2</sub> H <sub>4</sub>                   | Hydrazine                          |
| (NH <sub>4</sub> ) <sub>2</sub> SO <sub>4</sub> | Ammonium chloride                  |
| Ni  | Nickel                             |
| O <sub>2</sub>                                  | Oxygen                             |
| PA  | Polyacetylene                      |
| PANI  | Polyaniline                        |
| PE  | Polyethylene                       |
| PEDOT   | Poly(3,4-ethylene dioxthiophene)   |
| PMMA  | Poly(methylmethacrylate)           |
| PP  | Polypropylene                      |
| PPY   | Polypyrrole                        |
| PS  | Polystyrene                        |
| PTH   | Polythiophene                      |
| PVA   | Poly(vinyl alcohol)                |
| PVC   | Poly(vinyl chloride)               |
| Pt  | Platinum                           |
| rGO   | Reduced graphene oxide             |
| SAED  | Selected area electron diffraction |
| SDBS  | Sodium dodecylbenzene sulfonate    |
| SDS   | Sodium dodecyl sulphate            |
| SO <sub>2</sub>                                 | Sulphur dioxide                    |
| SEM   | Scanning electron microscopy       |
| XPS   | X-ray photoelectron spectroscopy   |
| XRD   | X-ray diffraction                  |
| UV-vis  | Ultraviolet-visible                |
| TEM   | Transmission electron microscopy   |

# **SINTESIS DAN PENCIRIAN POLIANILIN, GRAFIN DAN NANO KOMPOSIT GRAFIN/POLIANILIN**

## **ABSTRAK**

Kebelakangan ini, nanokomposit dengan grafin dan polimer konduktif telah menarik perhatian kerana kekonduksian elektriknyanya yang unggul. Tujuan utama kajian ini adalah untuk meningkatkan kekonduksian elektrik Polianilin (PANI) dengan penambahan grafin yang difungsikan. Objektif bagi kajian ini dibahagikan kepada dua bahagian. Dalam bahagian pertama, kesan penggunaan natrium dodekil benzenesulfonat (SDBS) sebagai surfaktan dan kaedah berbeza untuk menghasilkan PANI (konvensional fasa tunggal dan pempolimeran antara muka) telah dikaji. Dalam bahagian kedua, grafin telah dihasilkan melalui pengelupasan elektrokimia grafit dengan menggunakan voltan elektrokimia yang berbeza iaitu 5V dan 10V. Grafin/PANI-SDBS nanokomposit telah dihasilkan dengan melalui satu-langkah pempolimeran antara muka yang mudah dengan kandungan grafin yang berbeza. Keputusan menunjukkan bahawa nanogentian PANI yang seragam dengan diameter yang kecil (55 nm) dapat dihasilkan dengan menggunakan pempolimeran antara muka. Penambahan SDBS semasa pempolimeran antara muka PANI berjaya mengurangkan aglomerasi nanogentian PANI. Voltan yang rendah, 5V dapat menghasilkan grafin yang nipis dengan kecacatan yang rendah ( $I_D/I_G=0.36$ ), meningkatkan kestabilan terma serta kekonduksian elektrik yang tinggi iaitu  $2.53 \times 10^{-1}$  S/cm. Kajian morfologi menggunakan FESEM dan HRTEM menunjukkan bahawa nanogentian PANI cenderung untuk menyalut di atas permukaan grafin. Nanokomposit yang mengandungi 5% berat badan grafin telah menunjukkan kekonduksian elektrik yang paling tinggi iaitu  $2.53 \times 10^{-1}$  S/cm, dengan empat kali ganda lebih tinggi daripada PANI ( $9.99 \times 10^{-6}$  S/cm). Kestabilan terma dan kekonduksian elektrik nanokomposit telah meningkat bertambahnya kandungan grafin.

# **SYNTHESIS AND CHARACTERIZATION OF POLYANILINE, GRAPHENE AND GRAPHENE/POLYANILINE NANOCOMPOSITES**

## **ABSTRACT**

Recently, nanocomposites with graphene and conducting polymers have attracted considerable attention because of their superior electrical conductivity. The main aim of this study is to enhance electrical conductivity of polyaniline (PANI) by addition of functionalized graphene. The objectives of the present study are divided into two parts. In the first part, effect of using sodium dodecylbenzenesulfonate (SDBS) as surfactant and two different methods to synthesize PANI (conventional single-phase and interfacial polymerization) are considered in the study. In the second part, graphene were synthesized through electrochemical exfoliation of graphite with different electrochemical applied bias of 5V and 10V. The graphene/PANI-SDBS nanocomposites have been synthesized through a simple one-step interfacial polymerization by varying the amount of graphene content. Results indicate that more uniform with smaller diameter (55 nm) of PANI nanofibers are produced using interfacial polymerization. The growth of PANI nanofibers into agglomeration was successfully suppressed with the addition of SDBS during the interfacial polymerization of PANI. The low applied bias, 5V yields thin graphene sheets with relatively low defect ( $I_D/I_G=0.36$ ), enhanced thermal stability as well as show high electrical conductivity of  $2.53 \times 10^{-1}$  S/cm. The morphological analysis via field emission scanning (FESEM) and high resolution transmission electron microscopy (HRTEM) showed that PANI nanofibers tend to coat on the surfaces of graphene sheets. The nanocomposites containing 5 wt% graphene content exhibit the highest electrical conductivity of  $2.53 \times 10^{-1}$  S/cm, which is four orders of magnitude higher than that of PANI ( $9.99 \times 10^{-6}$  S/cm). The thermal stability and electrical conductivity of nanocomposites was found to be improved with the increased in graphene content.

## CHAPTER ONE

### INTRODUCTION

#### 1.1 Background of Research

Carbon nanomaterials including zero-dimensional (0-D) fullerenes, one-dimensional (1-D) carbon nanotubes (CNTs) and two-dimensional (2-D) graphene have been widely investigated due to their versatile characteristics and properties. Graphene, a two-dimensional honeycomb  $sp^2$  carbon lattice has received enormous attention in recent years for its potential application in next generation composite materials as well as electronic and energy storage devices. Graphene was considered as the basic unit for other carbon materials and it can be wrapped up into 0-D buckyballs, rolled into 1-D nanotubes or stacked into three-dimensional (3-D) graphite as shown in Figure 1.1. As opposed to other carbon nanomaterials, the special two dimensional structure makes graphene displays a number of unique material properties including large theoretical specific surface area ( $2630 \text{ m}^2\text{g}^{-1}$ ), high intrinsic mobility ( $200\,000 \text{ cm}^2\text{V}^{-1}\text{s}^{-1}$ ) (Bolotin *et al.*, 2008; Morozov *et al.*, 2008), high Young's modulus ( $\sim 1.0 \text{ TPa}$ ) (Lee *et al.*, 2008), superior thermal conductivity ( $\sim 5\,000 \text{ Wm}^{-1}\text{K}^{-1}$ ) (Balandin *et al.*, 2008), high optical transmittance and good electrical conductivity.

To date, several methods have been demonstrated for graphene synthesis using both top-down and bottom-up approaches. In recent years, mechanical exfoliation, chemical exfoliation, chemical synthesis and thermal chemical vapour deposition (CVD) synthesis are the most commonly used methods. Although mechanical exfoliation using scotch tape was the first method of synthesized graphene sheets by Geim and Novoselov in 2004 and this discovery igniting the field of graphene, but the

yield is limited (Chia *et al.*, 2014). A popular low-cost method to produce graphene in large quantities is obtained from chemical exfoliation of graphite via Hummers method. However, this process has the disadvantages with the resulting reduced graphene oxide (rGO) sheets having structural defects, giving poor quality in terms of low electrical conductivity which depends largely on removal of the functional groups through chemical or thermal reduction. Moreover, this method involves the usage of hazardous or corrosive chemicals (Liu *et al.*, 2015).

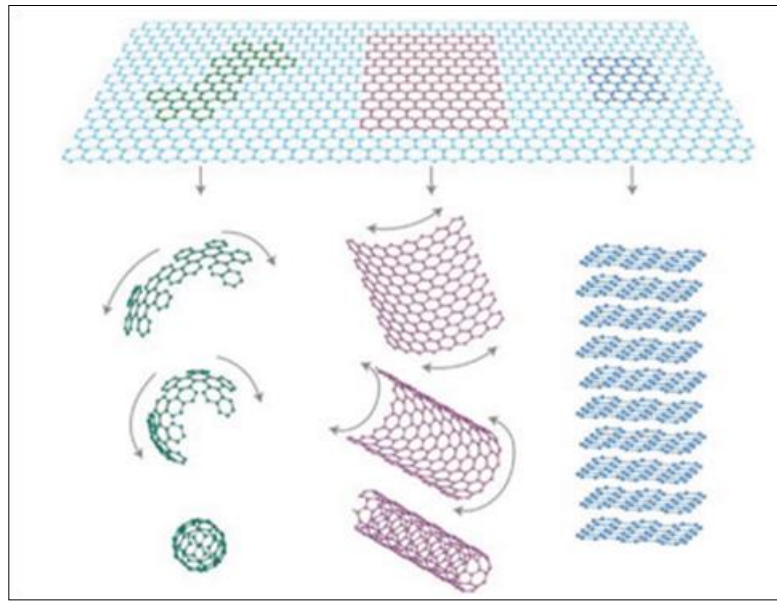


Figure 1.1: Graphene is a 2D building material for carbon materials of all other dimensionalities (Geim & Novoselov, 2007).

CVD method has been most widely used to grow large area graphene. However, this method requires the use of high temperature or expensive equipment process (Oyer *et al.*, 2012; Soldano *et al.*, 2010). Recently, the electrochemical method have drawn much attention and it is considered as a promising low-cost route for the mass production of graphene (Zhong *et al.*, 2015). This method takes several minutes to hours, producing gram scale quantities of graphene at the laboratory-scale. The quality of graphene is strongly affected by the operating voltages, graphite precursors and

electrolyte (Yang *et al.*, 2016). Electrochemical exfoliation of bulk graphite can generate graphene with a diverse range of characteristics.

There are still some challenges in order to utilize the great potential of graphene for various applications. It has been found that the graphene sheets tend to agglomerates and would result in insoluble in water and organic solvents due to the  $\pi$ - $\pi$  stacking interactions. In order to overcome this, functionalization of graphene such as chemically introduced a new functional groups onto the surface of graphene is considered as an approach to address the challenges. Moreover, the presence of hydrophilic groups such as carboxylic and sulfonate groups can be introduced onto the basal planes of graphene to prevent aggregation.

Graphene have shown a great promise in preparing the nano-scale sensors, conductors, capacitors, batteries and other (Huang *et al.*, 2012). In addition, one of the most significant applications of the graphene is to incorporate them into some polymers as the reinforcing fillers to synthesize nanocomposites. Organic polymers possess some limitations such as low thermal stability and poor mechanical, electrical and optical properties due to their intrinsic nature. The discovery of conducting polymers has generated a great interest in conductive nanocomposites. The most widely studied conducting polymers are polyaniline (PANI), polypyrrole (PPy) and poly(3,4-ethylene dioxthiophene) (PEDOT) (Flandin *et al.*, 2001).

Among the various conducting polymers, the PANI family of conjugated polymers has attracted much attention. Besides conductivities, PANI is favourable than other because the monomer aniline is less expensive and the synthesis of PANI is simple. Moreover, PANI has excellent environmental stability and tunable properties. Most recently, nanostructured PANI has received great potential because its